

# Evaluation of Geosynthetic-Reinforced Flexible Pavements using Static Plate Load Tests

John S. McCartney

*University of Colorado Boulder, USA*

Brady R. Cox, Clinton M. Wood, and Brandon Curry

*University of Arkansas at Fayetteville, USA*

**Keywords:** Pavement reinforcement, geogrids, geotextiles, plate load test

**ABSTRACT:** This study focuses on the response of full-scale geogrid-reinforced flexible pavements to static surface loading. Specifically, static plate load (SPL) tests were performed on a low-volume, asphalt pavement frontage road in Eastern Arkansas, USA (the Marked Tree Site). This site is among the most unique geosynthetic-reinforced pavement research sites in the USA, consisting of sixteen 15 m-long sections including different geosynthetic types, two base course thicknesses, and control sections. Maximum deflections under a maximum static surface stress of 540 kPa ranged from 2.5 to 4 mm. At least four unload-reload curves were obtained for each section to dampen the effects of the visco-elastic response of the asphalt surface layer on the system stiffness. The range in tangent stiffness obtained from the third reload cycle for the pavement sections ranged from 495 to 905 kPa/mm during the winter (dry season), and 452 to 725 kPa/mm during the late spring (wet season). A smaller decrease in stiffness from the wet season to the dry season was noted for the reinforced sections. The trends in the stiffness values indicate logical trends with reinforcement type and base course thickness, indicating that the SPL test is suitable for global characterization of the geosynthetic-reinforced sections. Three-layer elastic analyses using moduli determined using Spectral Analysis of Surface Waves (SASW) were found to be useful in quantifying the impact of geosynthetic reinforcement on the surface settlement. Although predicted elastic settlements were greater than measured settlements, the trends were similar. The Poisson's ratios of the base course layers in each section (incorporating the geosynthetic reinforcement as a composite) were found to be a useful parameter to account for the effect of geosynthetic reinforcement on the base lateral confinement.

## 1 BACKGROUND AND PURPOSE

Approximately 97% of paved roadways in the United States are flexible pavements, consisting of compacted soil surfaced with asphalt concrete (FHWA 1998). Flexible pavements are particularly subject to fatigue failure due to combined environmental interaction and vehicle loading. Environmental interaction will eventually lead to an increase in moisture content in the pavement base and subgrade soils, resulting in a decrease in compressive and shear moduli. Repeated vehicle loading under these weakened conditions can lead to rutting, fatigue cracking, and migration of fine particles (pumping) (Yoder and Witczak 1975). Degradation of flexible pavements has been addressed by installation of sub-drainage to dissipate pore water pressure in the pavement structure, installation of hydraulic barriers to limit the effects of environmental interaction, placement of a geotextile barrier between the subgrade and base soils to prevent intrusion of aggregate particles into

the subgrade (separation), use of lime to decrease the hydraulic conductivity of the soil and stabilize its volume change potential, and use of basal reinforcement with geosynthetics to aid in redistributing stresses imposed on the subgrade through the base. Out of these potential solutions, basal reinforcement with geosynthetics is gaining momentum due to observations of increased pavement performance, or the opportunity to reduce the amount of aggregate base to reach the same performance (Berg et al. 2000). This is combined with the ease of geosynthetic installation and the potential multi-functionality of some geosynthetics beyond reinforcement (e.g., separation or drainage).

Previous experience with basal reinforcement of pavements with geosynthetics consists primarily of empirical observations from a relatively limited number of full-scale case studies, and several full-scale test track and laboratory-scale box studies. Although many researchers indicate that basal reinforcement leads to improved pavement performance, a field testing method has not been identified to consistently quantify the contribution of the geosynthet-

ic to the pavement's overall performance. The Falling Weight Deflectometer (FWD) is the primary field test that has been used to quantify the global pavement resilient modulus (Kinney et al. 1998). However, the results from this test (i.e., the resilient modulus) do not permit transparent assessment of the geosynthetics' contribution. Due to the lack of a systematic evaluation of field tests for pavement section, the influence of different reinforcement materials used in of pavements has not been well characterized. The purpose of this study is to evaluate the feasibility of using static plate load tests as a characterization tool for reinforced pavements, as they are inexpensive and relatively simple to perform (Terzaghi 1955; Das 1992). Further, when combined with layered elastic analyses, surficial stress and deformation data from static plate load tests may be used to extract effects of the geosynthetic reinforcement on the overall pavement performance.

## 2 TEST SITE DESCRIPTION

A series of sixteen, 15-m long, geosynthetic-reinforced pavement test sections were constructed by the Arkansas State Highway and Transportation Department (AHTD) along the frontage road to Highway 63 in Marked Tree, AR in the summer of 2005 (Howard 2006). The original intention of the Marked Tree project was to evaluate the long-term impacts of traffic and subgrade-environment interaction on full-scale reinforced and unreinforced pavements. As such, the site was instrumented with H-type asphalt strain gauges, earth pressure cells (in both the base and subgrade), foil strain gauges bonded to the geosynthetics, and various environmental sensors (water content reflectometers, thermocouples, and a rain gauge) as a means to determine stress and strain distributions in the different pavement layers during high speed trafficking and environmental changes (Warren and Howard 2007). However, the instrumentation at the site was monitored for only a short time without significant trafficking or weather changes. Nonetheless, the Marked Tree Site presents a unique study area for geosynthetic-reinforced pavements due to the different geosynthetic reinforcement types, base course thicknesses, well-known geometry, and the availability of initial material properties.

A schematic of the 16 pavement test sections at the Marked Tree Site is shown in Figure 1. The average asphalt thickness across the test sections is 5.9 cm. The asphalt had a maximum theoretical specific gravity of 2.4 (Howard 2006). The base course was placed in two different thicknesses with a tapered transition section (Section 7) separating them. The base course material was crushed stone (AHTD class 7 aggregate), and was compacted using a vibratory roller to an average density of 2250 kg/m<sup>3</sup>. Sections

1b to 6 were constructed with approximately 25 cm of base, while Sections 8 to 13b were constructed with approximately 15 cm of base. Geosynthetics (woven and nonwoven geotextiles and geogrids) from three different manufacturers were installed at the site. The geosynthetic reinforcement, regardless of type, was placed directly on the subgrade soil. The subgrade at the site is poor and generally classifies as fat clay (CH) with an average PI of 42. Prior to construction, approximately 30 cm of surficial subgrade soil was homogenized and re-compacted to a dry density of 1860 kg/m<sup>3</sup>, corresponding to a soaked CBR of approximately 1.5 (Howard 2006). The sections with smaller base course thickness were constructed by compacting additional subgrade fill so that the surface of the final base course level was uniform at the end of construction.

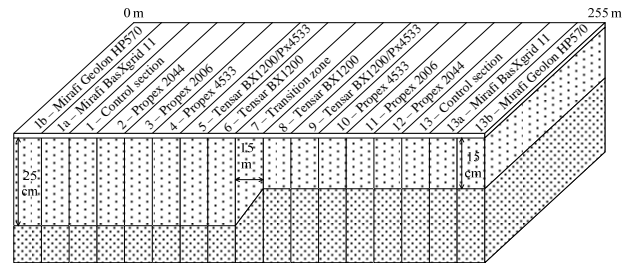


Fig. 1: Schematic of geosynthetic-reinforced pavement test sections at Marked Tree, AR.

Before performing the plate load tests, the average shear wave velocities of the three layers (asphalt, base course, and subgrade soil) were measured using Spectral Analysis of Surface Waves (SASW) (Stokoe and Santamarina 2000). Receiver spacings ranged from 7.6 to 121.6 cm were used for SASW measurements, which is consistent with SASW measurements on pavements used by Barfield (2007). The shear moduli values for each layer, shown in Figure 2 on a logarithmic scale, were calculated by multiplying the dry density of each pavement layer by the square of its shear wave velocity. Although there is some slight variability from section to section due to moisture content differences (for the base) and temperature (for the asphalt), these properties are relatively consistent from section to section.

The air temperature during the tests was approximately 1°C for the tests in December, while it was 30°C for the tests in May. The pavement temperature was approximately 4°C and 35°C in December 2008 and May 2009, respectively. The lower temperature likely led to higher stiffness values in the asphalt for the winter months. Measurements of the volumetric moisture content of the base and subgrade soils using capacitance probes indicate that the soils are unsaturated, with degree of saturations of 0.6 and 0.65 in December and May, respectively. The higher degree of saturation likely led to the lower moduli for the base course and subgrade in the spring.

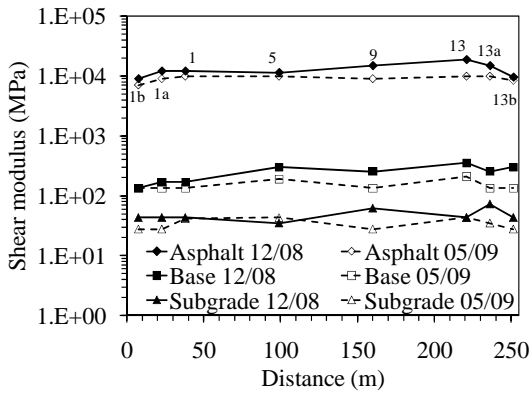


Fig. 2: Shear modulus values calculated using dry density values and SASW results

### 3 EXPERIMENTAL SETUP/PROCEDURES

A schematic view of the static plate load test setup is shown in Figure 3. Two DC Linear Variable Differential Transformers (LVDTs) were used to measure the dynamic surface deflection basin during testing. The support frame for the LVDTs is a 4.3 m-long aluminum support frame, which is intended to limit the effects of radial surface deformations. Aluminum was used as it has a lower coefficient of thermal expansion than steel. All tests were performed in 500 s, so the impact of thermal changes on deformation measurements was assumed to be negligible. A picture of the loading system and the LVDT support frame is shown in Figure 4.

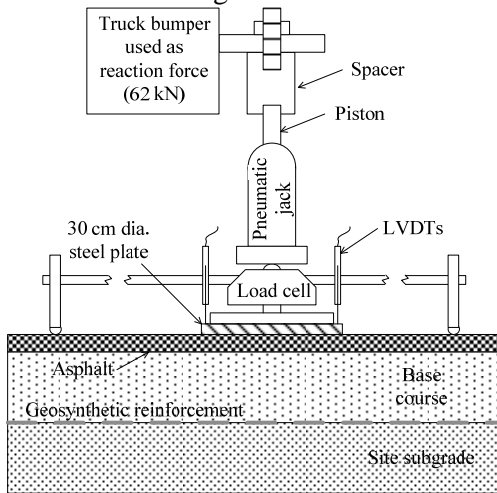


Fig. 3: Schematic of the static plate load setup and instrumentation layout

Static plate load tests were performed in eight of the sections at a distance of 4.5 meters away from the nest of embedded sensors. They were performed using an air compressor to supply a constant pressure to the pneumatic jack. The weight of the back-end of the truck (60 kN) was expected to be the maximum load applied, although loads closer to 45 kN were obtained during testing. Consistent with Terzaghi (1955), multiple loading cycles were applied to the ground surface by releasing the pressure and reloading. In contrast, the same maximum stress

was applied to the pavement surface after each loading cycle. This was intended to dampen out the effects of the visco-elastic creep in the asphalt layer on the load-settlement curves.

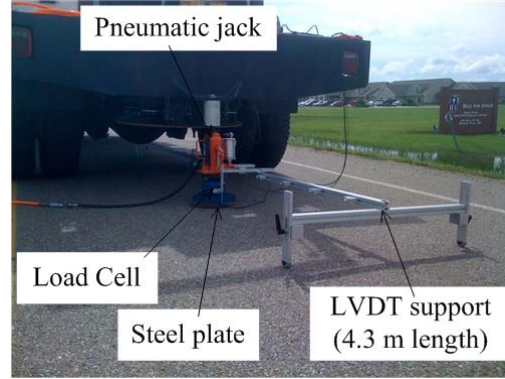


Fig. 4: Picture of the static plate load test

### 4 RESULTS

The time series of load and settlement obtained during a typical plate load test are shown in Figure 5. For each of the tested sections, at least four loading cycles were performed. This figure shows how the pavement did not rebound to the same level after each cycle due to time rate effects, and a slightly greater settlement was obtained during each cycle. Although not considered in this paper, the data showing the viscous rebound of the pavement surface observed during unloading can be considered to better characterize the properties of the asphalt layer.

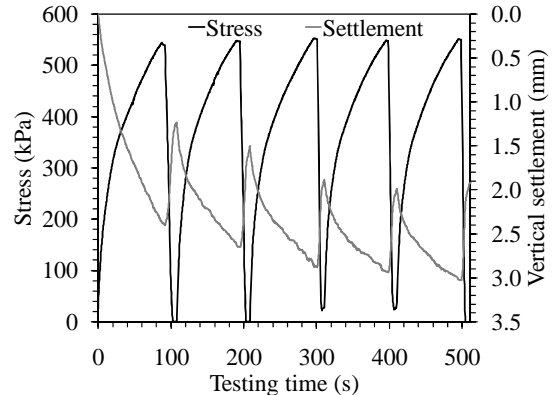


Fig. 5: Time series of applied surface stress and measured settlement (Section 13b)

The load settlement curve defined using the time series in Figure 5 is shown in Figure 6(a). This figure shows that the re-loading curves have a similar slope after each loading cycle, although there is some nonlinearity at stresses above 500 kPa. Even though the same load was applied on each cycle, some plastic deformation is noted after each cycle due to the visco-elastic creep of the asphalt. The stiffness values defined for each loading cycle in Figure 6(a) are shown in Figure 6(b). The stiffness was consistent during each reloading cycle, so the average value of the latter four cycles was used to define the stiffness of the pavement system.

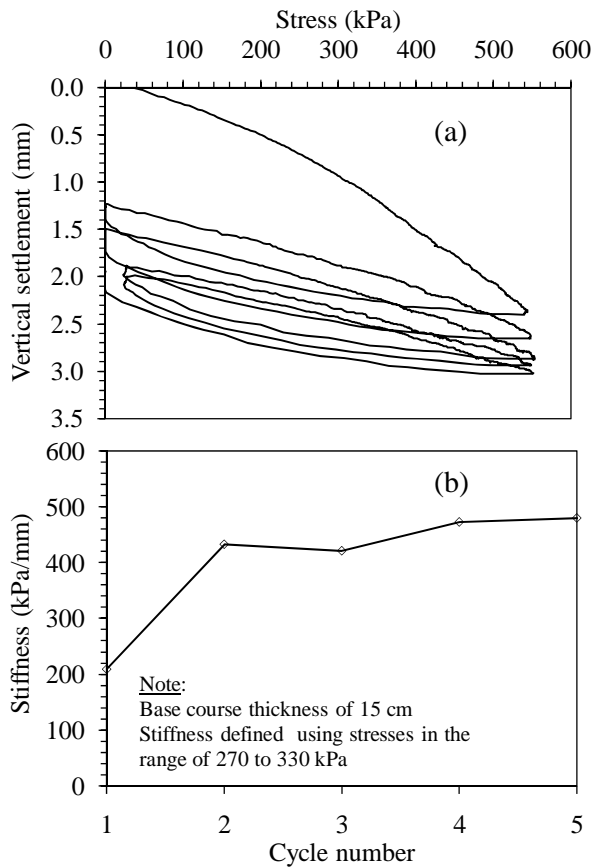


Fig. 6: Typical plate load test results for a geogrid-reinforced section (Section 13b): (a) Load-settlement curves; (b) Trend in stiffness with loading cycles

To define the surface stress values in Figure 6(b), it was necessary to select a range of surface stresses within which the soil layers beneath the asphalt experience a high enough stress level to mobilize strains at that level. Further, because there are two different base course sections at the site, it is important to define the stress ranges such that a fair comparison may be made between the stiffness values between these sections. The three-layer elastic stress distribution tables presented by Jones (1962) were used to calculate the stress at the base-subgrade interface. For a section with a 25 cm-thick base course, the vertical stress at the base-subgrade interface would be 50 kPa under a surface stress of 500 kPa (close to the maximum stress applied in all sections). To obtain the same stress at the base-subgrade interface in a section with a 15 cm-thick base course, a surface stress of only 300 kPa would need to be applied. Accordingly, a range of stresses of 450 to 550 kPa were used to define the stiffness of the sections with a 25 cm-thick base course, while a range of stresses of 270 to 330 was used to define the stiffness of the sections with a 15 cm-thick base course [as used in Figure 6(b)].

A similar approach was used to define the stiffness values for several of the other pavement sections at the Marked Tree site. The stiffness values measured during December 2008 (near freezing

conditions in the dry season), and during May 2009 (warm conditions in the wet season) are shown in Figure 7. The results show that the sections with a base course thickness of 15 mm generally have lower plate load stiffness than those with a base course thickness of 25 mm. In general, a decrease in pavement stiffness was noted from the winter to the spring. This is attributed to a loss in suction in the subgrade and base course soils due to environmental interaction during the wet season. In addition, the asphalt was nearly frozen during the winter tests, which also contributed to the stiffness. Despite using different ranges of stress to define the pavement stiffness, the pavement layers with a thinner base course section generally show a lower stiffness than those with thicker base course.

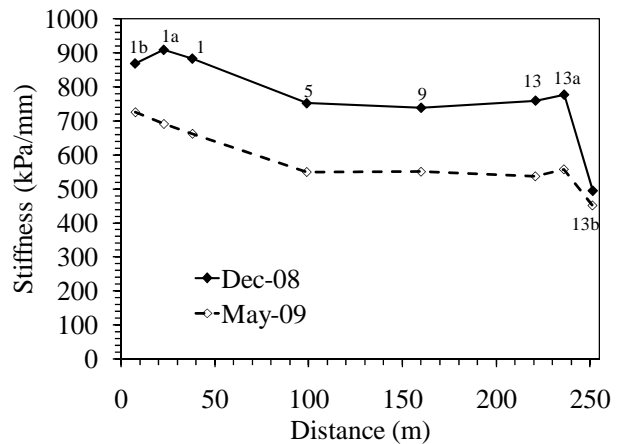


Fig. 7: Plate load stiffness values for the pavement sections (See Figure 1 for section types)

Out of all of the sections, the geogrid-reinforced sections (Sections 1a and 13a) showed the highest stiffness of the pavement sections grouped by base course thickness. However, the geosynthetic reinforced sections at times did not perform better than adjacent unreinforced sections (i.e., Sections 1a and 1, and Sections 13 and 13b). Comparing the trends in the layer moduli defined using SASW (Figure 2) with those in Figure 7 indicate that this observation may be due to the fact that the asphalt is stiffer in the unreinforced sections, as are the base and subgrade, than in the reinforced sections. This may have been due to construction variability (perhaps by an inadvertent effort to construct the control sections “well” so that they would be a fair comparison with the reinforced sections). An interesting observation from the results in Figure 7 is that the reinforced sections showed less of a decrease in stiffness from the dry season to the wet season when compared to the decrease in stiffness of the unreinforced sections (1 and 13). The sections with a geogrid placed atop a geotextile (Sections 5 and 9) were observed to perform as good as the unreinforced sections. Sections 5 performed worse than all of the other sections with a 25 cm-thick base course, while Section 9 performed as well as the other sections with a 15 cm-thick base course.

## 5 ANALYSIS

The goal of the analysis in this paper is to discern the effects of lateral restraint of a geosynthetic on the settlement of a reinforcement pavement under static loading. This analysis combines the measurements of layer moduli obtained using SASW with an elastic analysis. Vakili (2008) synthesized several linear elastic theories to determine the settlement of a layered system loaded using a rigid plate having a diameter  $a$  and a force  $q$ , given the elastic parameters of the individual layers. Vakili (2008) combined the analysis of Thenn de Barros (1966) with that of Palmer and Barber (1940). Thenn de Barros (1966) showed how the upper two layers in a three layer system shown in Figure 8 could be replaced by a single layer having an equivalent modulus  $E_e$  of:

$$E_e = \left( \frac{h_a^3 \sqrt{E_a} + h_b^3 \sqrt{E_b}}{h_a + h_b} \right)^3 \quad (1)$$

where  $h_a$  and  $h_b$  are the thicknesses of the asphalt and base course, respectively, and  $E_a$  and  $E_b$  are the Young's moduli of the asphalt and base course, respectively. Palmer and Barber (1940) showed that a two layer system can be replaced by a single layer of subgrade material having a Young's modulus of  $E_s$  and Poisson's ratio of  $\nu_s$ , but with a thickness of:

$$h_e = (h_a + h_b) \left( \frac{E_e(1 - \nu_s)^2}{E_s(1 - \nu_e)^2} \right)^{1/3} \quad (2)$$

A summary of how the layered systems are synthesized is shown in Figure 8. In this analysis, the properties of the base course and geosynthetic reinforcement are considered as a single composite material due to the small thickness of the geosynthetic.

Vakili (2008) calculated the vertical surface settlement  $W_z$  underneath the center of the footprint as:

$$W_z = \left( \frac{2(1 - \nu_s^3)qa}{E_s} \right) \left\{ \begin{array}{l} k^3 + (1 - k^3) \left[ \sqrt{1 + \left( \frac{m}{k} \right)^2} - \frac{m}{k} \right] \\ \times \left[ 1 + \frac{m}{2k(1 - \nu_s^3)} \sqrt{1 + \left( \frac{m}{k} \right)^2} \right] \end{array} \right\} \quad (3)$$

where the parameters  $m$  and  $k$  are equal to:

$$m = \frac{h_a + h_b}{a} \sqrt{\frac{1 - \nu_s^2}{1 - \nu_e^2}} \quad (4)$$

$$k = \sqrt[3]{\frac{E_s}{E_e}} \quad (5)$$

The surface settlements calculated using Equation (3) are shown in Figures 9 and 10 for tests performed in December 2008 and May 2009, respectively. Also shown in these figures are the settlement values calculated by dividing the applied stress  $q$  (500 kPa for the sections with a base course thickness of 25 cm and 300 kPa for the sections with a base course thickness of 15 cm) by the measured stiffness values shown in Figure 7.

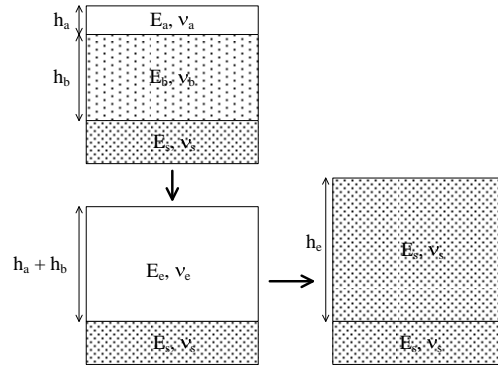


Fig. 8: Approach to combine pavement layers with equivalent elastic properties

The Young's moduli values in Equation (3) were calculated from the shear moduli measured using SASW combined with estimates of the Poisson's ratios of the different layers. Although the shear modulus data for the subgrade in Figure 2 shows variability the average shear modulus was used in the analysis (43 MPa for sections tested in December 2008 and 34 MPa for sections tested in May 2009). In this analysis, the Poisson's ratio of the subgrade soil was assumed to be 0.49 (undrained), while the Poisson's ratio for the asphalt was selected to be 0.33 based on tests performed by Howard (2007). The Poisson's ratio for the base course was adjusted so that the trends in the settlement values calculated using Equation (3) were consistent with those calculated using the measured stiffness values. The magnitudes of the measured settlements are relatively close to those calculated using Equation (3).

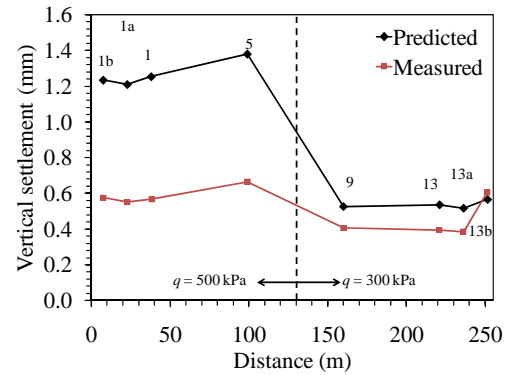


Fig. 9: Calculated and measured settlements for tests in December 2009

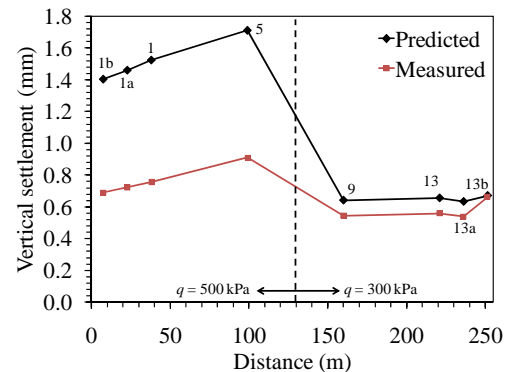


Fig. 10: Calculated and measured settlements for tests in May 2009

The Poisson's ratios that were defined in order to match the surface settlement data are shown in Figure 11. This variable proved to be a good indicator of the lateral restraint mechanism in reinforced pavements. In other words, the difference in vertical settlement is likely related to the lateral expansion of the different pavement layers during vertical loading. These results also indicate that the Poisson's ratio may be a function of the matric suction in the base course, which changes due to environmental interaction.

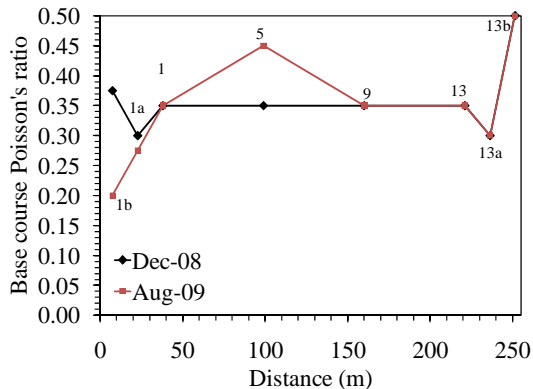


Fig. 11: Poisson's ratios for the base course layers defined to match trends in measured surface settlements for the different sections

## 6 CONCLUSIONS

This study shows that the SPL test is suitable for global characterization of the geosynthetic-reinforced sections. The range in tangent stiffness obtained from the third reload cycle for the pavement sections ranged from 495 to 905 kPa/mm during the winter (dry season), and 452 to 725 kPa/mm during the late spring (wet season). A smaller decrease in stiffness from the wet season to the dry season was noted for the reinforced sections. The trends in the stiffness values indicate logical trends with reinforcement type and base course thickness. Elastic analyses using moduli determined using Spectral Analysis of Surface Waves (SASW) were found to be useful in quantifying the impact of geosynthetic reinforcement on the surface settlement, using the Poisson's ratio of the base course as the main fitting parameter. The Poisson's ratio of the base course layer was found to be a useful parameter to account for the effect of geosynthetic reinforcement on the base lateral confinement.

## 7 ACKNOWLEDGEMENTS

The results in this paper are from project TRC-0903 funded by the Arkansas State Highway and Transportation Department. The contents in this paper reflect the views of the authors and do not necessarily reflect the views of the sponsor.

## 8 REFERENCES

- Barfield, O. (2007). "Mechanistic Procedure for Prediction of the In-Situ Resilient Modulus of Unbound Aggregate Base from Seismic Testing." M.S. Thesis. U. of Texas at Austin.
- Berg R., Christopher, B., and Perkins, S. (2000), Geosynthetic Reinforcement of the Aggregate Base Course of Flexible Pavement Structures, GMA White Paper II, Geosynthetic Materials Association, Roseville, MN, USA, 130p.
- Das, B. (1992). Principles of Soil Dynamics. PWS. Boston.
- Federal Highway Administration (FHWA). (1998). Assessing the Results of the Strategic Highway Research Program. Publication No. FHWA-SA-98-008. Washington D.C.
- Howard, I. (2006). "Low Volume Flexible Pavement Roads Reinforced with Geosynthetics." Doctoral Dissertation. The University of Arkansas at Fayetteville.
- Jones, A. (1962). "Table of Stresses in Three-Layer Elastic Systems." Highway Research Board Bulletin No. 342.
- Kinney, T.C., Stone, D.K. and Schuler, J. (1998). "Using Geogrids for Base Reinforcement as Measured by Falling Weight Deflectometer in Full-Scale Laboratory Study." TRR 1611, Washington, DC, pp. 70-77.
- Palmer, L. A. and Barber, E. S. (1940). "Soil Displacement under Circular Loaded Areas." Proc. Highway Research Board. 20, 279-286, 319-332.
- Warren, K. and Howard, I.L. (2007). "Sensor Selection, Installation, and Survivability in a Geosynthetic-Reinforced Flexible Pavement." Geosynthetics Int. 14(5), 299-315.
- Stokoe, K.H., II Wright, S.G., Bay, J.A. and Roesset, J.M. (1994). "Characterization of Geotechnical Sites by SASW Method." ISSMFE Tech. Committee #10 for XIII ICSMFE. Geophysical Characterization of Sites, Balkema. 15-25.
- Terzaghi, K. (1955) Evaluation of coefficient of subgrade reaction, Geotechnique. 5(4), 297-326.
- Thenn de Barros, S. (1966). "Deflection Factor Charts for Two and Three-Layer Elastic Systems." Highway Research Record. 145, 83-108.
- Vakili, J. (2008). "A Simplified Method for Evaluation of Pavement Layers Moduli Using Surface Deflection Data." The 12th Int. Conf. of Int. Assoc. for Comp. Methods and Adv. In Geomechanics (IACMAG). 1-6 Oct. Goa, India.
- Yoder, E. and Witzcak, A. (1975). "Principles of Pavement Design." John Wiley and Sons. NY.